ELSEVIER

Journal of Atmospheric and Solar-Terrestrial Physics 68 (2006) 769–780

Journal of ATMOSPHERIC AND SOLAR-TERRESTRIAL PHYSICS

www.elsevier.com/locate/jastp

Geomagnetic signatures during the intense geomagnetic storms of 29 October and 20 November 2003

S. Alex[a,*], S. Mukherjee[a], G.S. Lakhina[a,b]

[a]*Indian Institute of Geomagnetism, Plot No. 5, Sector-18, New Panvel(W), Navi Mumbai 410 218, India*
[b]*Research Institute for Sustainable Humanosphere, Kyoto University, Gokasho, Uji, Kyoto 611-0011, Japan*

Received 11 May 2005; received in revised form 24 November 2005; accepted 3 January 2006
Available online 20 February 2006

Abstract

Solar cycle 23 in its declining phase witnessed the most pronounced space weather events during October–November 2003. A series of powerful solar flares and associated geoeffective Coronal Mass Ejections (CMEs) travelling at ~2000 km/s drove shock fronts that impacted the Earth's magnetic field consecutively on 29 and 30 October, resulting in intense geomagnetic disturbances during 29–31 October. Another intense geomagnetic storm activity occurred during 20–21 November, resulting from a solar flare that had an associated geoeffective CME travelling at a speed of ~1100 km/s. Digital ground magnetic field measurements from the equatorial and low-latitude locations in the Indian longitude zone, in conjuction with the interplanetary solar wind and magnetic filed parameters, are used to study the characteristics of these storms. Maximum magnitude of the total magnetospheric energy injected into the magnetosphere during the mainphase of the three major storm amounts to approximately 4.5×10^{13}, 3.6×10^{13}, 2.8×10^{13} W. Another salient feature brought out is the close correspondence between the magnitude of the peak of the southward component of the interplanetary magnetic field B_z and the strength of the storm intensity as inferred from the D_{st} and low-latitude digital magnetic records.

Keywords: Geomagnetic storms; Ring current; Coronal mass ejections; Magnetospheric dissipation

1. Introduction

Solar flares and Coronal Mass Ejections (CMEs) are basic outbursts arising from the instabilities of the magnetic field in the tenuous solar atmosphere. Solar flares of severe intensity are associated with the evolution of sheared magnetic field occurring predominantly at locations of magnetically complex region of the Sun. CMEs are known as large-scale structures expelled from the closed coronal magnetic field regions of the Sun that overlie magnetic polarity inversion lines (Kahler, 1992; Hundhausen, 1993). The energetic radiations bursts from the flares on the Sun travel at the speed of light, and so arrive at Earth just 8 min after leaving the flare site, well ahead of any particle or coronal materials emanating from the Sun. CMEs are gigantic upward mass motions seen in the outer corona of the Sun that involves the ejection of very large quantities of plasma away from the Sun into the interplanetary space. A CME when released from the Sun's gravity travels faster than the solar wind giving rise to a

*Corresponding author. Tel.: +91 222 7480764; fax: +91 222 7480762.
E-mail address: salex@iigs.iigm.res.in (S. Alex).

1364-6826/$ - see front matter
doi:10.1016/j.jastp.2006.01.003

shock front. These strong interplanetary disturbances cause many non-recurrent geomagnetic storms (Gosling et al., 1991; Gosling, 1993; Tsurutani et al., 1988; Richardson et al., 2001) in the Earth's magnetosphere and ionosphere and subsequently produce intense auroral activity, satellite damage, transformer failures and tripping of power grids. However, the geoeffectiveness of the CMEs depends on the structure of the magnetic field carried by it and the orientation of Earth-directed mass ejection from the Sun striking the Earth's magnetosphere. Manifestation of geomagnetic storm phenomena observed in the ground magnetic records is the result of enhanced coupling of solar wind with the magnetosphere mainly due to magnetic reconnection between the southwardly directed IMF and northward magnetopause fields (Dungey, 1961; Gonzalez and Mozer, 1974). The crucial role of North–South component of IMF (B_z) in regulating the electrodynamic coupling mechanism of energy transfer to produce geomagnetic storms has been established by several studies (Gonzalez and Tsurutani, 1987; Gonzalez et al., 1989, 1994; Kamide et al., 1999; Wu and Lepping, 2002). A necessary and sufficient condition for the occurrence of major storms as laid down by Tsurutani and Gonzalez (1997) and Tsurutani et al. (1999) is the maintenance of a southward B_z of large magnitude above the normal field of -5 nT, for a sufficiently long period ($>\sim 3$ h or more). The earlier findings by Burlaga (1991), Tsurutani et al. (1992) also demonstrated the correspondence between majority of large magnetic storms and a class of transient solar ejecta called magnetic clouds. Typical magnetic storm characteristics are manifested as the depression in the horizontal component of the geomagnetic field known as the main phase, lasting for various time scales ranging from a few to almost 10 h or more and the slow recovery phase lasting about 1 to several days. The storm main phase is due to the enhanced westward ring current around the Earth at distances of around 2–8 R_E(1 R_E = 6378 km). At the decay of the ring current starts the storm recovery phase. The understanding of the detailed geomagnetic signatures of storm development and recovery under the variable solar activity conditions still remains a paradigm.

During intense solar activity, the electromagnetic and particle ejections from the Sun are dominated by flares and CMEs. Solar activity maximum years 2000 and 2001 witnessed several intense geomagnetic storms associated with CMEs. Solar cycle 23 had its Sunspot maximum in April 2000 but with a secondary peak occurring in November 2001. This explains the bimodal distribution of intense geomagnetic storms at two levels, a first peak during high solar activity and a secondary peak in the descending phase of the solar cycle. Solar cycle distribution of the geomagnetic storms has been dealt with by Gonzalez et al. (1990), describing the occurrence feature of dual peaks, with one peak occurring near or at solar maximum and the other at the descending phase. The powerful solar flares and CMEs that occurred during October–November 2003 clearly depict the geoeffective nature of the solar activity 2 years following the solar maximum. The present study investigates the ground magnetic field variations associated with the complex solar ejections on 28 October and 19 November 2003.

2. Methodology

The study uses the digital magnetic records from the equatorial station Tirunelveli (Geogr. 8°42′N, 77°48′E; Geomag. 0.36°S, 149.78°) and the low-latitude station Alibag (Geogr. 18°37′N, 72°52′E; Geomag. 9.7°N, 145.6°) in conjunction with the available parameters of solar wind and interplanetary magnetic field from the satellites. Solar wind data from the Advanced Composition Explorer (ACE)/Solar Heliospheric Observatory (SOHO) at L_1 point and the Geotail at $X\sim 3\,R_E$ during the events are the satellite database used to highlight the salient features of the shock events. The solar activity conditions were obtained from the *Report and Forecast of Solar Geophysical Data*.

3. Flare, CME and the geoeffectiveness of the shock

3.1. X17 flare and CME on 28 October 2003

The Sunspot group 486 (S17E04) became active on 26 October 2003 giving rise to the eruption of a series of X-class flares. This region developed into a giant Sunspot at 1110 UT on 28 October emitting a powerful solar flare of X17/4B magnitude. NOAA had reported the region 486 as one of the largest and most complex active regions of solar cycle 23. The Mass Time-of-Flight spectrometer (MTOF) sensor of NASA/ESA's SOHO (~1 AU) reported a saturated maximum detectable speed by the proton monitor of 1100 km/s from 0600 UT on 29 October to 2000 UT on 30 October 2003. Solar wind detectors onboard the NASA's ACE spacecraft located at the L_1 Langrangian point (~240 R_E, 1 R_E = 6378 km) were contaminated due to the large proton events following the intense flare activity. Hence the plasma data were available with gaps. The Large Angle and Spectrometric Coronagraph (LASCO) instrument onboard SOHO observed an Earthward directed full halo CME on 28 October streaming at a fast speed of ~2000 km/s. The X17 flare event at 1110 UT on 28 October produced proton events >10 MeV at 1215 UT and almost 1 h later the proton event >100 MeV occurred. This proton event was characterized by a proton flux unit of 29 500 pfu, which is the second largest event after the largest proton event in November 2001 of the present solar cycle. In terms of the high-speed events, CMEs of 29 and 30 October 2003 as the third fastest to reach the Earth in 19 h (Skoug et al., 2004). The earlier recorded fastest events are the 4 August 1972 and the great storm of 2 September 1859, with transit times of the CMEs identified as 14.6 h and 17.5 h, respectively.

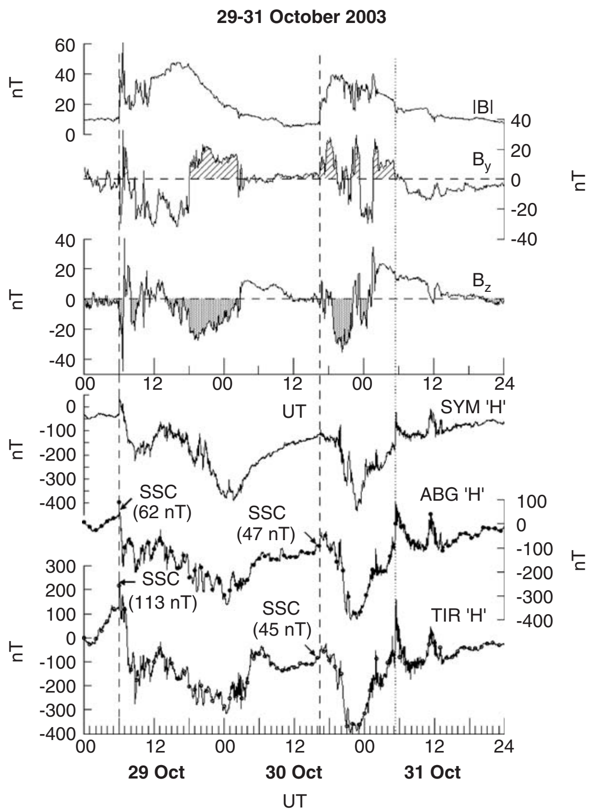

Fig. 1. Interplanetary magnetic field parameters (ACE) of the magnetic storm events during 29–31 October 2003. Vertical dashed lines indicate the arrival of the first shock at ACE at 0600 UT on 29 October and the second shock at 1600 UT on 30 October 2003. The arrows show SSC's at Alibag (ABG) and Tirunelveli (TIR) at 0612 UT on 29 October and 1620 UT on 30 October 2003. The SSC amplitudes are given in parenthesis. The 1 min data of SYM 'H' and the magnetic field data of the 'H' component of ABG and TIR are time shifted by 12 min to correspond to the interplanetary shock arrival on 29 October 2003. The shaded portion marked by slanted lines show intervals of northward B_y and the dotted portion represents southward B_z.

The solar wind monitoring satellites SOHO/ACE detected the arrival of a large high-speed solar wind shock front at 0600 UT on 29 October 2003. As mentioned earlier, the transit time of the CME passage from the Sun to the SOHO/ACE location was about 19 h, thereby rating this event as a significantly large storm in this solar cycle 23. The large shock front impacted the Earth's magnetic field near instantaneously to produce the geomagnetic storm sudden commencement at 0612 UT, as shown by a vertical dashed line in Fig. 1. The vertical dashed line corresponds to the arrival time of shock, for which the time is shifted for the ground magnetic records with respect to the shock at 0600 UT on 29 October. The geostationary satellites GOES 10, 11, 12 experienced magnetopause crossings and went outside of the magnetosphere for a period of more than 10 h after the onset of this severe storm.

3.2. *X10 flare and CME on 29 October 2003*

Active region 486 (S17W09) unleashed another major flare of X10/2b at 2049 UT on 29 October as recorded by GOES X-ray flux (1–8 Å) data. NOAA also reported the intense radio emissions accompanied by the flare. Due to the X10 flare, a secondary enhancement in the continuing proton events of >10 and >100 MeV were observed late on the 29 October. This eruption also hurled a cloud matter (CME) at a speed of almost 1950 km/s directed towards the Earth as reported in the *Report and Forecast of Solar Geophysical Data*. Solar wind detectors onboard the NASA's ACE spacecraft located at the L_1 point were contaminated due to the large proton events following the intense flare activity thereby making the data unreliable. The second severe impact was detected by solar wind monitoring satellite with the arrival of a shock front at 1600 UT on 30 October that impacted the magnetosphere 20 min later giving rise to the sudden commencement of a geomagnetic storm (Fig. 1).

3.3. M3.2 flare and CME on 18 November 2003

Subsequent to the highly disturbance phenomena of October, complex series of flares and associated full halo CME that occurred on 18 November produced an intense geomagnetic storm on 20 November. Sunspot region 501 (N00E18) produced a M3.2/2N flare at 0723 UT on 18 November. The speed of the associated CME was estimated at 1100 km/s. The shock arrived at the L1 point as reported by SOHO/ACE at 0740 UT on 20 November which gave rise to an enhancement of 40 nT at 0803 UT in the 'H' component of the magnetic field at the low-latitude station, Alibag. Table 1 summarizes the main characteristics of the solar events that led to the intense geomagnetic storms in October–November 2003.

4. Magnetospheric response

The main characteristics of a geomagnetic storm, is represented by the quantitative measure of the disturbance of the H component from selected observatories at low latitude and distributed over longitudes. D_{st} index is being considered as a measure of the ring current intensity and its energy (Suguira, 1964).

Variations in the solar wind pressure contribute to the perturbations in the magnetic field variations recorded on the ground. Burton et al. (1975) were the first to incorporate the correction factor to remove the magnetopause current contribution from the measured D_{st}, by the expression, $D^*_{st} = D_{st} - b\sqrt{P} + c$, where P is the solar wind dynamic pressure, b and c are constants and D^*_{st} the pressure corrected D_{st}. Different studies have obtained certain variable values for the constants. In the present study, we have adopted the correction factors as given by Gonzalez et al. (1994).

Table 1
Solar events associated with the three largest geomagnetic storms of 2003

Solar event	29 October	30 October	20 November
Solar flare	X17/4b	X10/2b	M3.2/2N
Occurrence	28 October/ 1110 UT	29 October/ 2049 UT	18 November/ 0723 UT
CME speed (km/s)	~2000	~1950	~1100
Transit time (h)	19 h	19 h	48 h
Solar source	S17E04	S17W09	N00E18
Proton events (MeV)	>10, >100	>10, >100	>2
Shock at 1 AU (UT)	0600	1600	0740
V_{sw} at 1 AU (m/s)	~1850	~1710	~750
D^*_{st} (nT)	−358	−406	−491

The interplanetary energy flux parameter epsilon (ε) was introduced by Perrault and Akasofu (1978), which is a quantity representing the solar wind energy entering into the magnetosphere. The ε function is related to the Poynting flux and it is highly dependent on the solar wind velocity and the magnitude and direction of the interplanetary magnetic field. The ε function, which gives an estimate of the total energy transferred into the magnetosphere, can be written as (Perrault and Akasofu, 1978; Nishida, 1983)

$$\varepsilon = vB^2 \sin^4(\theta/2) l_o^2, \tag{1}$$

where v is the upstream solar wind speed, B the magnitude of the IMF, θ the IMF clock angle defined as $\theta = \tan^{-1}(|B_y/B_z|)$ for $B_z > 0$, and $\theta = 180^\circ - \tan^{-1}(|B_y/B_z|)$ for $B_z < 0$, i.e., the polar angle of the IMF projected on the Y–Z plane, l_o is empirically determined value of the merging region at the subsolar magnetopause, assumed to be 7 R_E (Perrault and Akasofu, 1978; Akasofu, 1981).

Considering that the radius of the dayside magnetopause depends on the solar wind dynamic pressure, Mac-Mahon and Gonzalez (1997) replaced the distance l_o by the Chapman–Ferraro distance, R_{CF}, of the dayside magnetopause obtained from the balance between the kinetic plasma pressure of the solar wind and the magnetic pressure of the magnetosphere (Holzer and Slavin, 1979; Sibeck et al., 1991):

$$R_{CF} = (B_o^2/4\pi\rho v^2)^{1/6} R_E, \tag{2}$$

where B_o is the magnetic field strength on the surface of the Earth at the equator.

5. Storm–energy computations

In the computation of the total energy budget for the three major storms considered in the study, we have made use of the following energy equations. As the solar wind parameters were mostly saturated, kinetic energy of the solar wind for the major storm of October could not be computed.

The strength of the disturbance field is given by the Dessler Parker–Sckopke relationship between D_{st} and the energy of the ring current (Dessler and Parker, 1959; Sckopke, 1966). The Dessler Parker–Sckopke relation states that the magnetic perturbation caused by ring current particles is directly proportional to their total energy. Russell et al. (1974) demonstrated the development of the ring current in response to the southward turning of the interplanetary magnetic field. Perrault and Akasofu (1978) and Akasofu (1981) expressed the quantitative estimate of the total magnetospheric energy consumption rate by the quantity U_T, expressed as the sum of the three major terms, i.e.,

$$U_T = U_R + U_J + U_A, \tag{3}$$

where U_R is the ring current injection rate, U_J is the power of Joule heating rate in the high-latitude ionosphere and U_A is the power consumption due to auroral particle precipitation.

Akasofu (1981) showed that the estimate of the ring current energy consumption, U_R, can be expressed in terms of the pressure corrected ring current index, D^*_{st}, as

$$U_R = 4 \times 10^{13}(\partial D^*_{st}/\partial t + D^*_{st}/\tau)\,(\mathrm{W}), \tag{4}$$

where $\partial D_{st}*/\partial t$ is the rate of change of D^*_{st}, D^*_{st} is the average value of pressure corrected D_{st}, and τ is the ring current life time in seconds.

Various researchers have adopted different procedures for evaluating the decay parameter, τ (Gonzalez et al., 1989; Alexeev et al., 1996; Mac-Mahon and Gonzalez, 1997; Kamide et al., 1998a, b). In the present work, we have used the function suggested by Valdivia et al. (1996) with modified D_{st} (D^*_{st}) to compute the value of τ for individual storm conditions.

The formula used in our present study for the computation of the power associated with the Joule heating U_J is by Ostgaard et al. (2002) that accounts for the summer asymmetry obtained by Ahn et al. (1989) and winter asymmetry obtained by Richmond (1990) in both the hemispheres:

$$U_J = (0.54\,\mathrm{AE} + 1.8) \times 10^9\,(\mathrm{W}). \tag{5}$$

Spiro et al. (1982) proposed the energy consumption by the auroral particle precipitation in both the hemispheres as given by

$$U_A = [1.75 \times (\mathrm{AE}/100 + 1.6)] \times 10^{10}\,(\mathrm{W}). \tag{6}$$

6. Observations and results

The top three panels in Fig. 1 show the magnitude of the interplanetary magnetic field |B| and its components B_y and B_z measured by ACE. Variations of the SYM 'H' component of the ring current along with the 'H' component of the geomagnetic field recorded at Alibag (represented as ABG 'H') and Tirunelveli (represented as TIR 'H') for the period 29 October to 31 October 2003 are presented in the bottom three panels.

The powerful CME from the X17/4b flare on 28 October at 1110 UT impacted the Earth's magnetosphere at 0612 UT on 29 October, subsequent to the shock observed by ACE and SOHO at 0600 UT.

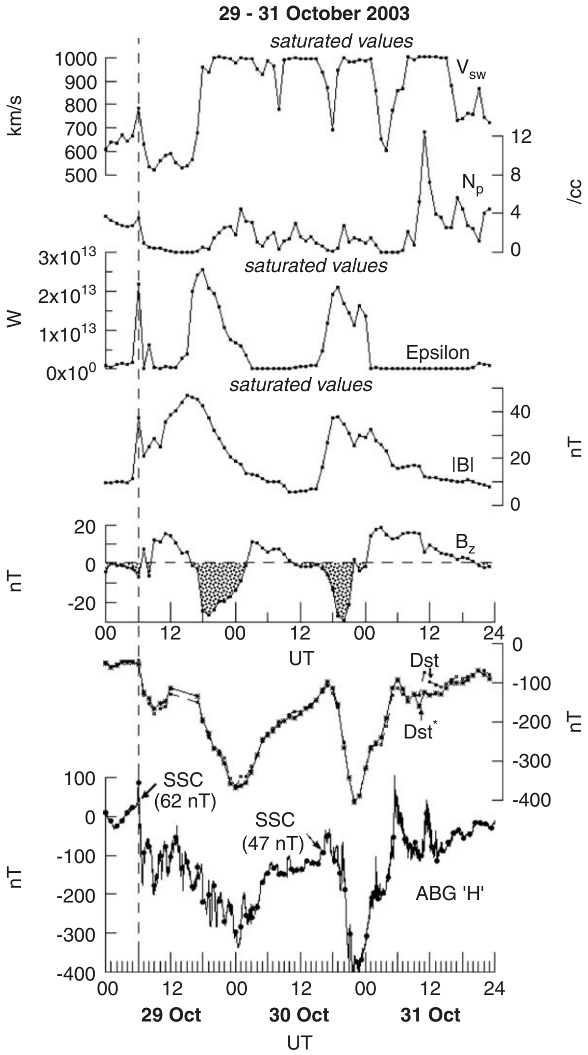

Fig. 2. Solar wind and interplanetary magnetic field parameters (ACE) of the magnetic storm events during 29–31 October 2003. The respective growth of the main phase during the two SSC's on 29 and 30 October 2003 are seen from the pressure corrected D_{st} index (D^*_{st}) and D_{st}. The magnetospheric energy input parameter, ε, for the two storm events is also shown. The one minute magnetic field data of the 'H' component of ABG is time shifted by 12 min to correspond to the interplanetary shock arrival at 0600 UT indicated by vertical dashed line on 29 October 2003.

The magnitude of the sudden impulse as seen in the storm sudden commencement in the 'H' component at the equatorial station Tirunelveli is 113 nT, and at the low-latitude station Alibag is 62 nT. The enhanced magnitude at the equatorial station is the influence of the noontime equatorial electrojet, the time of sudden commencement being 1100 LT for the location. Three hourly storm activity index '*K*' was 9 during the period of initial severe storming from 0600 to 0900 UT.

Continuous observations of the solar wind velocity (V_{sw}) and the proton number density (N_P) from SOHO/ACE at the L_1 point could not be recorded due to the degradation of the satellites electronics (Fig. 2, top two panels). However, the observations of the alpha particle speeds from Solar Wind Ion Composition Spectrometer (SWICS) instrument onboard ACE spacecraft during 29–30 October, indicated solar wind speeds exceeding 1900 km/s.

6.1. Storm main phase development (29–30 October)

Sharp increase in the interplanetary magnetic field $|B|$ (Fig. 1) from ACE/MAG around 0600 UT is seen as a two-step augmentation (40/60 nT) followed by highly fluctuating large B_z and B_y field prevalent at the moment of shock passage for a period of 1 h until 0700 UT. The interplanetary magnetic field polarity remained northward during the CME passage for sustained periods during the initial part of the main phase. This condition of the interplanetary environment might have led to the suppression in the overall intensity of the geomagnetic storm as evidenced from the ground magnetic records of 29 October as shown in the bottom panel of Fig. 1. The fluctuating negative B_z in the first part of the storm during 0600–0900 UT on 29 October has produced favourable conditions for geomagnetic storm occurrence. During this period of highly modulating interplanetary magnetic field, the ground magnetic variations of the 'H' component at Tirunelveli and Alibag also showed fluctuating negative magnetic fields. However, the oscillating field magnitude tends to become less negative when the interplanetary magnetic field B_z becomes positive but keeps on modulating during the period 0900–1300 UT. Thus the development of intense main phase was inhibited during fluctuating northward B_z. When the interplanetary magnetic field component B_z turned southward again, the main phase depression restarted with the decrease of ground magnetic field at the two stations (1300–2400 UT). The storm development in this event clearly follows a double storm signature. This is in conformation with the ideas put forth by Kamide et al. (1998a, b), suggesting that an intense storm can result from the superposition of two successive moderate storms, driven by two successive southward B_z. However, starting from 1800 UT onwards sharp and steady southward B_z seemed to persist for almost 6 h favourable for intense geomagnetic storm occurrence. The peak intensity in the disturbance occurred at 2400 UT to a level of ~350 nT in D_{st}, following which a slow recovery of this storm started when a steady rotation of the B_z field occurred. A gradual decrease in the interplanetary magnetic field $|B|$ is also evident from the curve in the top panel, wherein a steady field of about 10 nT remained from 0600 to 1500 UT on 30 October. The onset of another severe storm followed this calm condition. The fast CME from the X10 flare on 29 October at 2049 UT produced a shock that impacted the Earth's magnetosphere and gave rise to an enhancement in the 'H' component of the Earth's magnetic field at 1620 UT on 30 October 2003 (2nd SSC marked in the lower panel of Fig. 1). The magnitude of the storm sudden commencement as observed in the low-latitude magnetic record of Alibag on 30 October at this local nighttime is 47 and 45 nT for the equatorial station, Tirunelveli.

Unlike the storm main phase of 29 October, the development of a sharp main phase (D_{st}~−400 nT) commenced at 1800 UT on 30 October, as the southward B_z suddenly increased to −30 nT. Prior to this prominent southward directed field, B_z remained near zero and fluctuated for almost 2 h with albeit small magnitude. Abrupt turning of the B_z to northward direction around 2100 UT resulted in the beginning of the recovery, but the N–S modulation in the interplanetary magnetic field persisted until 0130 UT on 31 October.

In Fig. 2 are presented the solar wind parameters V_{sw} and N_p from the ACE satellite. Most of the time, V_{sw} values were saturated at the maximum of ~1000 km/s but the plot is provided to give an idea about the extreme conditions of the solar wind for the remarkable event of 29–31 October 2003. Hourly variation trend in the interplanetary magnetic field parameters $|B|$ and B_z are also shown in the middle block. All the points marked are hourly points, as the values of D_{st} index available were only hourly values. The pressure corrected D_{st} parameter, D^*_{st}, is also plotted along with D_{st}. Since the solar wind velocity (V_{sw}) and the proton number density (N_p) by ACE and WIND satellites could not be accurately estimated due to contamination in the satellite data, the values of epsilon as shown for the major storm are underestimated. The peaked values in the epsilon corresponding to the maximum magnitude of southward B_z during the two storm main phases on 29 and 31 October are of the order of 4.5×10^{13} W for the first main phase and 3.6×10^{13} W for the second main phase, respectively. Having discussed the geomagnetic effects during the storm development period and main phase period, the recovery of the storm of 31 October is seen to have occurred with the northward turning of the B_z field. After the field had returned to a level of -100 nT at Alibag on 31 October around 0500 UT, sudden rise in the H component is observed for almost 6 h with multiple peaks at 0500 and 1100 UT, though the second peak is not of large magnitude. This enhancement in the magnetic field is due to the occurrence of an interplanetary shock at 0451 UT. The corresponding solar wind parameters are given in Fig. 3 to elaborate the connection between the shock phenomenon and the ground magnetic signatures at low latitudes.

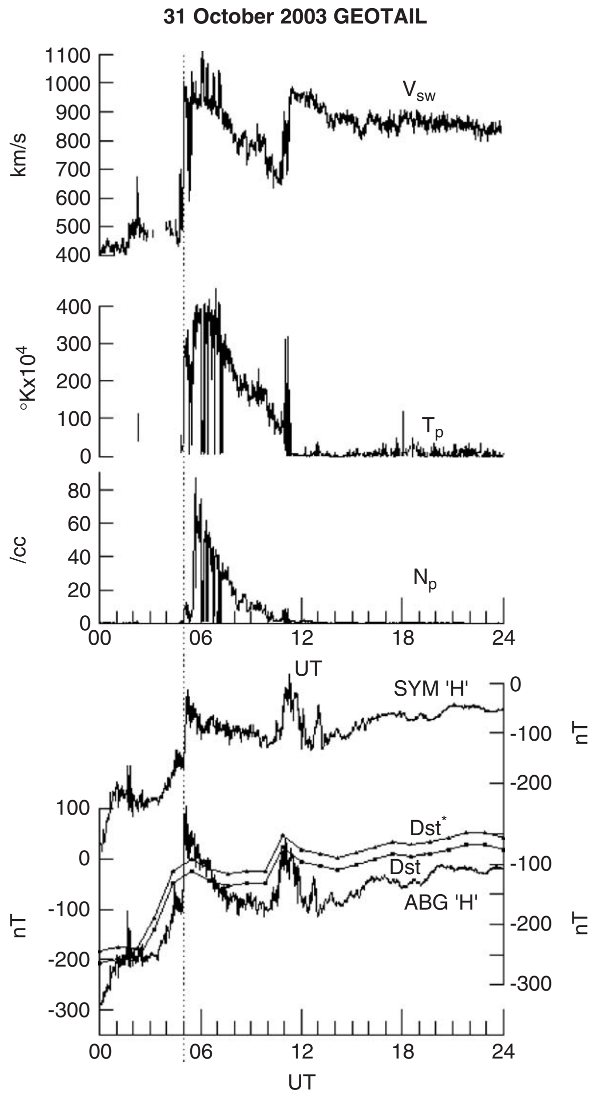

Fig. 3. Solar wind parameters from the Geotail satellite on 31 October 2003. Vertical dotted line indicates the interplanetary shock arrival at 0451 UT. Bottom panel shows SYM 'H', D^*_{st} and D_{st} (hourly) superimposed on the 1 min 'H' component magnetic field data of Alibag (ABG).

Referring to Fig. 3, evidence of an enhanced field is seen at 0500 and around 1100 UT and is of noticeable magnitude in all the geomagnetic parameters, viz. 1 min digital magnetic data from Alibag, 1 min SYM '*H*', D_{st} (WDC, Kyoto) and D^*_{st}. V_{sw}, T_p and N_p data from Geotail are shown, as the continuous data for the period were available from this satellite, which was located inside the magnetopause region. Large magnitude of the solar wind velocity, the number density and the proton temperature associated with the interplanetary shock produce large peaking in the 'H' component of the geomagnetic field. Fig. 3 depicts the shock phenomena at the time of recovery and its one to one correspondence with the low-latitude geomagnetic field.

6.2. Storm main phase development (20 November)

On 18 November a pair of M-class flares occurred and was accompanied by CMEs with approximate speed of 1100 km/s. A shock from the CME was observed to increase the solar wind speed from 350 to above 700 km/s as recorded at SOHO. Fig. 4 depicts the variation in interplanetary magnetic field parameters $|B|$, B_y and B_z from ACE/MAG and the variation in the horizontal component of the magnetic field, as observed from the 1 min digital data of the stations Tirunelveli and Alibag. At the time of the shock, at 0740 UT at the ACE location at $\sim$240 R_E, the ambient field increase was from 5 to 20 nT. Compression in the magnetic field associated with the CME passage produced a SSC enhancement of 40 nT at Alibag and 100 nT at the equatorial station Tirunelveli. The polarity of the magnetic field remained predominantly northward

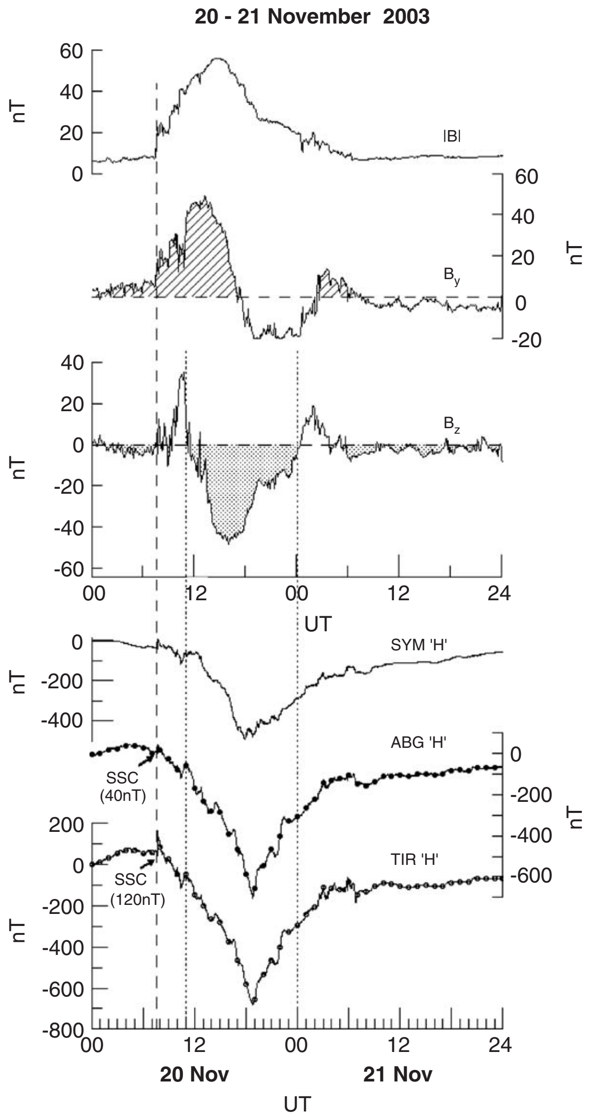

Fig. 4. Interplanetary magnetic field parameters (ACE) during the magnetic storm events on 20–21 November 2003. Vertical dashed line indicates the shock at 0740 UT. The arrows show the occurrence of SSC at 0803 UT at Alibag and Tirunelveli. The 1 min data of SYM 'H' and the magnetic field data of the 'H' component of Alibag and Tirunelveli are time shifted by 23 min.

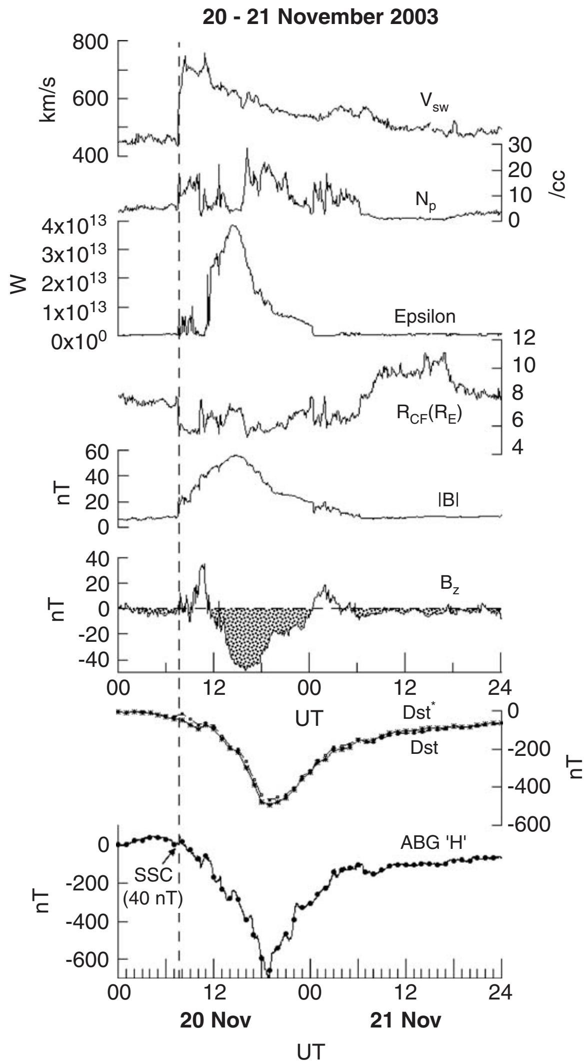

Fig. 5. Solar wind and interplanetary magnetic field parameters from ACE satellite during the magnetic storm events on 20–21 November 2003. The magnetospheric energy input coupling parameter, ε and the radius of the dayside magnetopause (R_{CF}) are shown. Pressure corrected D_{st} index parameter D^*_{st} and D_{st} shows correspondence with the magnetic field data of the 'H' component of Alibag which is time shifted by 23 min.

for a period of 4 h, after which the large southward turning of the B_z became prominent and significantly large magnitude of nearly -50 nT is seen. Corresponding magnetic field minimum is evident at the two locations Alibag and Tirunelveli (lower panel in Fig. 4) while $D_{st}\sim-500$ nT is as shown in Fig. 5. With the sharp rotation of the B_z to northward at 1800 UT, the ground magnetic field begins to recover as evident in Fig. 4. In Fig. 5 are also shown the solar wind velocity V_{sw}, proton number density N_p, the interplanetary magnetic field components from ACE alongwith the radius of the dayside magnetopause (R_{CF}) computed for the event and the magnetospheric energy input parameter epsilon (ε). Fig. 5 clearly shows that the value of R_{CF} parameter, i.e., the magnetopause distance, can become as small as about 5 R_E during the storm mainphase. For the October event, due to the saturated condition of the recordings of the solar wind parameters the R_{CF} values could not be done accurately.

7. Discussion and conclusions

Even though the CME associated with 28 October 2003 solar activity was so intense to saturate the recording of the solar wind parameters on board spacecraft at L_1 point, it failed to produce an equally intense storm feature in the magnetic records, as the interplanetary magnetic field was mostly northward oriented during the initial stretch of the shock process. However, it gave rise to pulsating variations of the ground magnetic field on 29 October which, more or less, followed the corresponding fluctuating and strong interplanetary magnetic field behind the large pressure gradient of the prime shock at 0600 UT. This remarkable feature observed in the initial development stage of the storm with modulating pattern in the 'H' component at Alibag and B_z, for the time interval 0615–1400 UT is shown in Fig. 6. Lag time of 25 min in the disturbance 'H' component at Alibag is considered for this plot. The scatter plot shows the close correspondence for the extreme values of B_z and the dips in the disturbance 'H' component. The circled points in the figure indicate the points of coincidence between intense negative B_z peaks(viz. −31.1 nT at 0625 UT, −48.2 nT at 0630 UT and −21.1 nT at 0835 UT) and the Alibag 'H' minimum values(viz. −182.9, −214.1 and −212.3 nT). It can be concluded that the 25 min lag corresponds to the response time of the magnetosphere to the interplanetary driving.

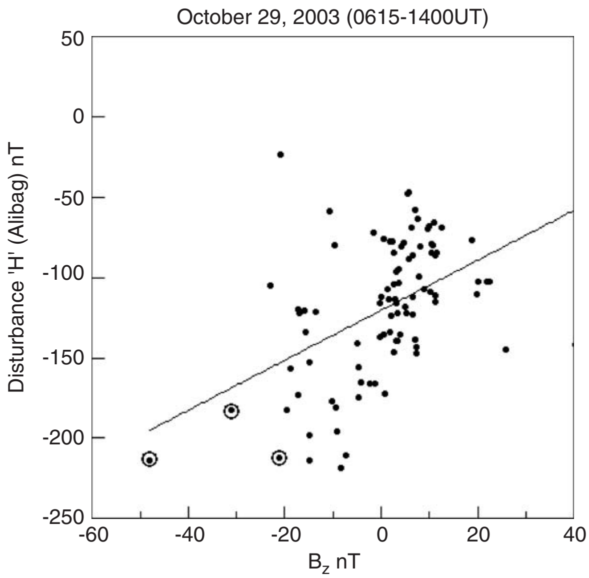

Fig. 6. Scatter plot using disturbance 'H' component (5 min) of the magnetic field at Alibag and the corresponding interplanetary magnetic field parameter B_z for the time period of 0615–1400 UT during the magnetic storm of 29 October 2003.

7.1. Energetics of the storms

Table 2a elaborates the magnitudes of the interplanetary and solar wind parameters from ACE satellite, magnitude of the planetary indices D_{st} and AE representing the ring current intensity and the Auroral Electrojet respectively. Comparative estimates of the calculated energy budgets are also shown (Table 2a) explicitly for the three storm mainphase periods, viz. magnetospheric energy input parameter ε, ring current energy injection rate U_R, energy dissipation due to auroral precipitation U_A, and the power of Joule heating U_J. The proportionality in the energy dissipation through

Table 2a
Energy budget for the three intense storm events in 2003

	29 October	30 October	20 November
SSC onset (UT)	06:12	16:20	08:03
SSC amplitude (nT) at TIR	113	45	120
SSC amplitude (nT) at ABG	62	47	40
IMF B_Z min (nT)/UT	−27/1809	−32.5/1904	−48/1520
Duration of southward IMF B_Z (h)	10	6	12
D^*_{st} min (nT)	−358	−406	−491
Main phase duration (h)	7	5	8
AE max (nT)	3800	3250	3000
V_{SW} (km/s)	1400	1700	585
N_P (/cc)	Saturated values	Saturated values	22
ε (GW)	45 320	35 869	28 259
U_A (GW)	693	597	553
U_J (GW)	2054	1757	1622
U_R (GW)	794	1086	1140
$U_T = U_A + U_J + U_R$ (GW)	3541	3440	3315

The values of ε computed are instantaneous values for maximum magnitude of southward B_z and the corresponding speed of the solar wind alpha particles taken from ACE Solar Wind Ion Composition Spectrometer (ACE/SWICS) Instrument (Skoug et al., 2004).

Table 2b
Proportionality in the energy dissipation for the three storm events in 2003

	29 October	30 October	20 November
U_T (GW)	3541	3440	3315
U_T/ε (%)	7.8	9.6	11.7
U_A/ε (%)	1.5	1.7	2.0
U_J/ε (%)	4.5	4.9	5.7
U_R/ε (%)	1.8	3.0	4.0

auroral precipitation, Joule heating and ring current intensification with respect to the magnetospheric energy input coupling parameter are also shown in Table 2b.

On 29–30 October, the unusually high solar wind speeds exceeded the energy range of the Solar Wind Electron Proton Alpha Monitor (SWEPAM) instrument onboard the ACE spacecraft thereby measuring saturated values. The ACE/SWEPAM also measured saturated values of proton density. The instantaneous values of the speed of solar wind alpha particles taken from ACE/SWICS alpha monitor (Skoug et al., 2004) corresponding to the maximum magnitude of the southward B_z component were used to compute the energy coupling parameter. For the storm on 29 October, at 18:09 UT corresponding to the time when the southward turning of the B_z was maximum, the computed energy coupling parameter ε is of magnitude 4.5×10^{13} W. On 30 October, the maximum magnitude of the energy coupling parameter ε computed is 3.6×10^{13} W at 1904 UT while for the storm on 20 November, the value of southward B_z peaked at 1520 UT and the energy coupling function ε amounted to be 2.8×10^{13} W.

The total energy consumption is computed from Eq. (3). The energies computed for the three storm events given in Table 2a, show that for the storm on 29 October, the magnetosphere–ionosphere system dissipated an average energy of 3.54×10^{12} W. Of this, 0.69×10^{12} W i.e. ~20% went into auroral precipitation, the contribution towards Joule heating was 2.05×10^{12} W i.e. ~58% and the ring current injection accounted for 0.79×10^{12} W i.e. 22%. For the storm on 30 October, the energy dissipated was of an average of 3.44×10^{12} W. From this total energy dissipated, auroral precipitation accounted for 0.6×10^{12} W, i.e. ~17%, Joule heating accounted for 1.76×10^{12} W, i.e. ~51% and the ring current injection was 1.1×10^{12} W, i.e. ~32%. Similarly for the storm on 20 November, the energy dissipated was of an average of 3.3×10^{12} W, the energy consumed as auroral precipitation was 0.55×10^{12} W, i.e. ~17%, Joule heating consumption was 1.6×10^{12} W, i.e. ~49% and ring current injection was 1.1×10^{12} W, i.e. ~33%. The estimate of the energy dissipation towards Joule heating is found to be 58%, 51% and 49% whereas the ring current consumption is much less being 22%, 32% and 33%, respectively, for the three storms. The mean maximum power in the ring current injection for the three storm main phase periods are 7×10^{11}, 10×10^{11} and 11×10^{11} W, respectively. Weiss et al. (1992) reported that even during intense storms ring current power rate has value of nearly 6×10^{11} W only. Modification in the magnitude of the ring current energy is known to have a clear dependence on τ. In the present study, computation of U_R has made use of the decay rate estimate computed by the equation of Valdivia et al. (1996). Resultant estimate of the energy injection rate suggests the efficiency of the reconnection process and further development of intense magnetic storms, which is known to be controlled to a large extent by the southward interplanetary magnetic field rather than the solar wind speed (Tsurutani et al., 1992; Gonzalez et al., 1989, 2002).

The total energy (U_T) dissipated by the magnetosphere–ionosphere system in all the three cases were almost the same order of magnitude, $\sim 3 \times 10^{12}$ W. However, the percentage of the total energy dissipated and the energy coupling from the solar wind estimated by the magnetospheric energy input parameter, ε, are very different. Moreover, Joule heating rate has shown substantially large magnitude of about 50% in case of all the three intense storms. Knipp et al. (1998) dealt in the manifestation and the development of consecutive major space storms during the descending phase of solar cycle 22 where they had closely examined the near Earth manifestations of prolonged high-speed streams during November 2–11, 1993. Our results have clearly shown that the major contribution to Joule heating is about 50% of the total consumption, the same is in conformity with the findings of Lu et al. (1998), Knipp et al. (1998), Koskinen and Tanskanen (2002) and Tanskanen et al. (2002).

It is clearly evident that the percentage proportionality of the energy dissipation and the magnetospheric energy input coupling parameter are in close correlation to the strength of the ring current as given by the magnitude of D_{st}. Close correspondence between the D_{st} magnitudes −358 , −406 and

−491 nT and the maximum southward B_z values for the three storms −27, −32 and −48 nT, respectively, attributes the occurrence of an intense mainphase of −491 nT for the storm of November 20 where B_z had a relatively large value (and remained southward for the largest duration of ~12 h).

The ratios of the energy dissipated with respect to the solar wind energy input into the magnetosphere bears significantly low values as is given in Table 2(b). Further, it is seen that U_T can account for about 10% of the total energy input during the three storms studied here. It appears that major portion goes into the field aligned currents, tail currents and the reconfiguration of the magnetosphere–ionosphere system. Baker et al. (2001) have dealt with various magnitudes of energy depositions for several geomagnetic storms wherein they have clearly stated the predominant role of energy dissipation to almost all parts of the magnetosphere and ionosphere with the dissipation occurring at different time scales for major storms. The results of Baker et al. (2001) on the progression in the magnetospheric energy dissipation with increase in the activity are quite relevant in the context of the present study.

Acknowledgements

The authors acknowledge CELIAS/MTOF experiment on the Solar Heliospheric Observatory (SOHO) spacecraft for providing the solar wind and the interplanetary parameters. SOHO is a joint European Space Agency (ESA) and United States National Aeronautics and Space Administration (NASA) mission. We thank the ACE SWEPAM instrument team and the ACE Science Center for providing the ACE data. We are thankful to the GEOTAIL mission project undertaken by the Institute of Space and Astronautical Science (ISAS) and NASA for providing the interplanetary parameters and also acknowledge the information from the Space Environment Center, Boulder, CO, National Oceanic and Atmospheric Administration (NOAA), US Deptartment of Commerce. We also thank WDC, Kyoto, for providing the preliminary Quick look AE, AL and AU, D_{st} and SYM-H indices. G.S. Lakhina would like to thank H. Matsumoto and Y. Omura for the kind hospitality during his stay at RISH, Kyoto University. The authors thank the reviewers for their encouraging comments.

References

Ahn, B.H., Kroehl, H.W., Kamide, Y., Gorney, D.J., 1989. Estimation of ionospheric electrodynamic parameters using ionospheric conductance deduced from Bremsstrahlung X-ray image data. Journal of Geophysical Research 94, 2565–2586.

Akasofu, S.I., 1981. Energy coupling between the solar wind and the magnetosphere. Space Science Review 28, 121–190.

Alexeev, I.I., Belenkaya, E.S., Kalegaev, V.V., Feldstein, Y.I., Grafe, A., 1996. Magnetic storms and magnetotail currents. Journal of Geophysical Research 101, 7737–7747.

Baker, D.N., Turner, N.E., Pulkkinen, T.I., 2001. Energy transport and dissipation in the magnetosphere during geomagnetic storms. Journal of Atmospheric and Solar-Terrestrial Physics 63, 421.

Burlaga, L.F., 1991. Intermittent turbulence in the solar wind. Journal of Geophysical Research 96, 5847–5851.

Burton, R.K., McPherron, R.L., Russell, C.T., 1975. An empirical relationship between interplanetary conditions and D_{st}. Journal of Geophysical Research 80, 4204–4214.

Dessler, A.J., Parker, E.N., 1959. Hydromagnetic theory of magnetic storms. Journal of Geophysical Research 64, 2239–2259.

Dungey, J.W., 1961. Interplanetary magnetic field and the auroral zones. Physical Review Letters 6, 47.

Gonzalez, W.D., Mozer, F.S., 1974. A quantitative model for the potential resulting from reconnection with an arbitrary interplanetary magnetic field. Journal of Geophysical Research 79, 4186–4194.

Gonzalez, W.D., Tsurutani, B.T., 1987. Criteria of interplanetary parameters causing intense magnetic storms ($D_{st} < -100$ nT). Planetary Space Science 35, 1101–1109.

Gonzalez, W.D., Tsurutani, B.T., Gonzalez, A.L.C., Smith, E.J., Tang, F., Akasofu, S.I., 1989. Solar wind magnetosphere coupling during intense magnetic storms (1978–1979). Journal of Geophysical Research 94, 8835–8851.

Gonzalez, W.D., Gonzalez, A.L.C., Tsurutani, B.T., 1990. Dual-peak solar cycle distribution of intense geomagnetic storms. Planetary Space Science 38, 181–187.

Gonzalez, W.D., Joselyn, J.A., Kamide, Y., Kroehl, H.W., Rostoker, G., Tsurutani, B.T., Vasyliunas, V.W., 1994. What is geomagnetic storm? Journal of Geophysical Research 99, 5771–5792.

Gonzalez, W.D., Tsurutani, B.T., Lepping, R.P., Schwenn, R., 2002. Interplanetary phenomena associated with very intense geomagnetic storms. Journal of Atmospheric and Solar-Terrestrial Physics 64, 173–181.

Gosling, J.T., 1993. The solar flare Myth. Journal of Geophysical Research 98, 18937–18949.

Gosling, J.T., McComas, D.J., Phillips, J.L., Bame, J., 1991. Geomagnetic activity associated with Earth passage coronal mass ejections. Journal of Geophysical Research 96, 7831–7839.

Holzer, R.E., Slavin, J.A., 1979. Magnetic flux transfer associated with expansions and contractions of the dayside magnetosphere. Journal of Geophysical Research 83, 3831.

Hundhausen, A.J., 1993. Sizes and locations of coronal mass ejections: 1993, SMM observations from 1980 and 1984–1989. Journal of Geophysical Research 98, 13177–13200.

Kahler, S.W., 1992. Solar flares and coronal mass ejections. Annual Review of Astronomy and Astrophysics 30, 113–141.

Kamide, Y., Yokoyama, N., Gonzalez, W.D., Tsurutani, B.T., Daglis, I.A., Brakke, A., Masuda, S., 1998a. Two-step development of geomagnetic storms. Journal of Geophysical Research 103 (A4), 6917–6921.

Kamide, Y., Baumjohann, W., Daglis, I.A., Gonzalez, W.D., Grande, M., Joselyn, J.A., McPherron, R.L., Phillips, J.L., Reeves, E.G.D., Rostoker, G., Sharma, A.S., Singer, J.Z., Tsurutani, B.T., Vasyliunas, V.M., 1998b. Two-step development of geomagnetic storms. Journal of Geophysical Research 103 (A8), 17705–17728.

Kamide, Y., Gonzalez, W.D., Vasyliunas, V.M., Tsurutani, B.T., McPherron, R.L., Rostoker, G., Phillips, J., Baumjohann, W., Joselyn, J.A., Sharma, A.S., Daglis, I.A., 1999. Comment on "Current understanding of magnetic storms—storm–substorm relationships". Journal of Geophysical Research 104, 7051.

Knipp, D.J., Emery, B.A., Engebreston, N., Li, X., McAllister, A.H., Mukai, T., Kokuban, S., Reeves, G.D., Evans, D., Obara, T., Pi, X., Rosenberg, T., Weatermax, A., McHarg, M.G., Chun, F., Mosely, K., Crodescu, M., Lanzerotti, L., Rich, F.J., Sharber, J., Wilkinson, P., 1998. An overview of the early November 1993 geomagnetic storm. Journal of Geophysical Research 103, 26197–26220.

Koskinen, H.E.J., Tanskanen, E.I., 2002. Magnetospheric energy budget and the epsilon parameter. Journal of Geophysical Research 107 (A11), 1415–1424.

Lu, G., Baker, D.N., Mcpherran, R.L., Farrugia, C.J., et al., 1998. Global energy deposition during the January 1997 magnetic cloud event. Journal of Geophysical Research 103, 11685–11694.

Mac-Mahon, R.M., Gonzalez, W.D., 1997. Energetics during the main phase of geomagnetic superstorms. Journal of Geophysical Research 102, 14199–14207.

Nishida, A., 1983. IMF control of the Earth's magnetosphere. Space Science Review 34, 185–200.

Ostgaard, N., Germany, G., Stadsnes, J., Vondrak, R.R., 2002. Energy analysis of substorms based on remote sensing techniques, solar wind measurements and geomagnetic indices. Journal of Geophysical Research 107 (A9), 1233.

Perrault, P., Akasofu, S.I., 1978. A study of magnetic storms. Geophysical Journal of Royal Astronomical Society 54, 547–573.

Richardson, I.G., Cliver, E.W., Cane, H.V., 2001. Sources of geomagnetic storms for solar minimum and maximum conditions during 1972–2000. Geophysical Research Letters 28, 2569–2572.

Richmond, A.D., 1990. Global measures of ionospheric electrodynamic activity inferred from combined incoherent scatter radar and ground magnetometer observations. Journal of Geophysical Research 95, 1061.

Russell, C.T., Mcpherron, R.L., Burton, R.K., 1974. On the cause of geomagnetic storm. Journal of Geophysical Research 79 (7), 1105–1109.

Sckopke, N., 1966. A general relation between the energy of trapped particles and the disturbance field near the Earth. Journal of Geophysical Research 71, 3125.

Sibeck, D.G., Lopez, R.E., Roelof, E.C., 1991. Solar wind control of the magnetopause shape, location and motion. Journal of Geophysical Research 96, 5489.

Skoug, R.M., Gosling, J.T., Steinberg, J.T., McComas, D. J., Smith, C.W., Ness, N.F., Hu, Q., Burlaga, L.F., 2004. Extremely high speed solar wind: 29–30 October 2003. Journal of Geophysical Research 109, A09102.

Spiro, R.W., Reiff, P.H., Maher, L.J., 1982. Precipitating electron energy flux and auroral zone conductances: an empirical model. Journal of Geophysical Research 87, 8215–8227.

Sugiura, M., 1964. Hourly values of equatorial D_{st} for the IGY. Annual International Geophysical Year 35, 945–948.

Tanskanen, E.I., Pulkinen, T.I., Koskinen, H.E.J., Slavin, J.A., 2002. Substorm energy budget during low and high solar activity: 1997 and 1998 compared. Journal of Geophysical Research 107 (A6), 1086–1097.

Tsurutani, B.T., Gonzalez, W.D., 1997. The interplanetary causes of magnetic storms; a review. In: Tsurutani, B.T., Gonzalez, W.D., Kamide, Y. (Eds.), Magnetic storms. Geophysical Monograph Series, 98, AGU, Washington, DC, pp. 77–90.

Tsurutani, B.T., Gonzalez, W.D., Tang, F., Akasofu, S.I., Smith, E.J., 1988. Origin of interplanetary southward magnetic field responsible for major magnetic storms near solar maximum (1978–1979). Journal of Geophysical Research 93, 8519–8531.

Tsurutani, B.T., Gonzalez, W.D., Tang, F., Lee, Y.T., 1992. Great magnetic storms. Geophysical Research Letters 19, 73–76.

Tsurutani, B.T., Kamide, Y., Gonzalez, W.D., Lepping, R.P., 1999. Interplanetary causes of great and superintense magnetic storms. Physics and Chemistry of the Earth 24, 101.

Valdivia, J.A., Sharma, A.S., Papadopoulos, K., 1996. Prediction of magnetic storms by nonlinear dynamical models. Geophysical Research Letters 23, 2899–2902.

Weiss, L.A., Reiff, P.H., Moses, J.J., Moore, B.D., Heelis, R.A., 1992. Energy dissipation in substorms. European Space Agency Special Publication ESA- SP 335, 309–319.

Wu, C., Lepping, R.P., 2002. Effects of magnetic clouds on the occurrence of geomagnetic storms: the first four years of WIND. Journal of Geophysical Research 107 (A10), 1314.